Journal of the American Heart Association

ORIGINAL RESEARCH

Transcriptome Analysis Identified *SPP1*-Positive Monocytes as a Key in Extracellular Matrix Formation in Thrombi

Takaya Kitano, MD, PhD; Tsutomu Sasaki, MD, PhD; Takahiro Matsui, MD, PhD; Masaharu Kohara, MSc; Kotaro Ogawa, MD, PhD; Kenichi Todo, MD, PhD; Hajime Nakamura, MD, PhD; Yuri Sugiura, MD; Yuki Shimada, MD; Shuhei Okazaki, MD, PhD; Junichi Iida, MD, PhD; Kohki Shimazu, MD; Eiichi Morii, MD, PhD; Manabu Sakaguchi, MD, PhD; Masami Nishio, MD, PhD; Masaru Yokoe, MD, PhD; Haruhiko Kishima, MD, PhD; Hideki Mochizuki, MD, PhD

BACKGROUND: Thrombi follow various natural courses. They are known to become harder over time and may persist long term; some of them can also undergo early spontaneous dissolution and disappearance. Hindering thrombus stability may contribute to the treatment of thrombosis and the prevention of embolisms. However, the detailed mechanisms underlying thrombus maturation remain unclear.

METHODS: We compared the RNA expression in 3 thrombi retrieved from cerebral vessels via thrombectomy with that in simultaneously sampled blood. The results were validated using immunohistochemistry on 66 thrombi retrieved from patients with cerebral embolism. Single-cell RNA sequencing data of thrombi from pulmonary arteries were used to uncover the molecular mechanisms.

RESULTS: A total of 1121 genes were upregulated in thrombi. Pathway enrichment and protein–protein interaction analyses revealed upregulation of extracellular matrix formation and identified *SPP1* as a hub gene. Immunohistochemistry revealed that expression level of osteopontin (the transcript of *SPP1*) positively correlated to that of collagen type VI in thrombi. Osteopontin was expressed primarily by monocytes/macrophages in the thrombi, particularly in older ones. Among these 66 patients, the presence of collagen type VI in the thrombus was marginally associated with longer puncture-to-reperfusion time and more passes before reperfusion, indicating that those thrombi were resistant to thrombectomy. Single-cell RNA sequencing of thrombi identified a subpopulation of monocytes/macrophages that highly express *SPP1*. These *SPP1*-high monocytes/macrophages highly expressed genes related to the extracellular matrix and communicated closely with fibroblasts.

CONCLUSIONS: Collectively, our findings indicate that *SPP1*-high monocytes/macrophages play a crucial role in thrombus maturation.

Key Words: extracellular matrix ■ osteopontin ■ RNA sequencing ■ stroke ■ thrombosis

Thromboembolic diseases account for 1 in every 4 deaths worldwide.[1] These diseases can be classified into 2 groups on the basis of whether the thrombus is formed in high- or low-pressure systems,[2] with intracardiac (cardiac atria) and venous thrombi accounting for most of the latter. Cardiogenic embolism,

Correspondence to: Tsutomu Sasaki, Department of Neurology, The University of Osaka Graduate School of Medicine, Osaka, Japan. Email: sasaki@neurol.med.osaka-u.ac.jp

This manuscript was sent to Daniel T. Eitzman, MD, Senior Guest Editor, for review by expert referees, editorial decision, and final disposition.

Preprint posted on bioRxiv May 29, 2024. https://doi.org/10.1101/2024.05.28.594130.

Supplemental Material is available at https://www.ahajournals.org/doi/suppl/10.1161/JAHA.125.044299

For Sources of Funding and Disclosures, see page 14.

JAHA is available at: www.ahajournals.org/journal/jaha

CLINICAL PERSPECTIVE

What Is New?

- Transcriptome analysis of human thrombi identified *SPP1*-positive monocytes as key contributors to extracellular matrix formation within thrombi, with osteopontin (encoded by *SPP1*) expression being associated with thrombus organization.

What Are the Clinical Implications?

- *SPP1*-positive monocytes represent a potential biomarker for thrombus age and organization, which may inform decisions regarding mechanical thrombectomy or thrombolytic therapy.
- Targeting *SPP1*-driven ECM remodeling may provide a novel therapeutic strategy to prevent thrombus stabilization.

Nonstandard Abbreviations and Acronyms

COL6	collagen type VI
CTEPH	chronic thromboembolic pulmonary hypertension
DEG	differentially expressed gene
ECM	extracellular matrix
PAI-1	plasminogen activator inhibitor-1
scRNA-seq	single-cell RNA sequencing

which can be caused by the embolism of an intracardiac thrombus, is the most severe type of ischemic stroke. Prevention of cardiogenic embolism is of significant interest because the number of patients with atrial fibrillation, the largest risk factor for cardiogenic embolism, is rapidly increasing worldwide.[3] Venous thrombi primarily form in the lower extremities and can be symptomatic. In some patients, these thrombi can embolize the pulmonary artery, which can be fatal. Anticoagulants are primarily used to prevent and treat thromboembolic diseases under low-pressure systems. Anticoagulants can decrease the risk of cardioembolic stroke in patients with atrial fibrillation; however, an approximate stroke risk of 40% remains even with anticoagulant treatment.[4] In addition, patients may experience bleeding complications.[5] Therefore, more effective antithrombotic therapies with low risk of bleeding are required.

Thrombi detected in patients can either disappear or persist. More than half (63%–89%) of thrombi found in atrial appendages disappear without symptomatic embolic events, whereas some patients develop cerebral embolism.[6–9] Moreover, 35% of surgery-associated venous thrombi resolve spontaneously within 72 hours, whereas some extend to involve the proximal veins.[10,11] Furthermore, half of pulmonary embolisms resolve within a few weeks, whereas thrombi persist; chronic thromboembolic pulmonary hypertension (CTEPH) occurs in ≈5% of patients after pulmonary embolism.[11,12] In recent studies, dynamic changes occurring in thrombi over time have been noted,[13,14] which may be involved in determining their natural course. As time passes after a deep venous thrombus is formed, the proportion of red blood cells decreases and the level of extracellular matrix (ECM) proteins, such as collagen, increases.[14] Thrombi can become stiffer and more resistant to thrombolysis over time.[15,16] Our research group and others have previously reported that older thrombi are more resistant to reperfusion therapy in patients with cerebral embolism.[17–19] Therefore, it can be assumed that conflicting processes occur within a formed thrombus: Some occur to make it stiff and stable and others to dissolve it. However, the mechanisms underlying these processes are not completely understood.

Here, we report the transcriptional differences between thrombi retrieved from cerebral vessels and peripheral blood. Our data identified *SPP1* as an upregulated hub gene for ECM formation in the thrombus, supported by immunohistochemistry analyses demonstrating positive correlation between *SPP1* transcript and collagen type 6 (COL6) expression. Furthermore, through single-cell RNA sequencing (scRNA-seq) data, our results indicate that *SPP1*-high monocytes and macrophagesare key players in ECM formation in thrombi. Collectively, our findings provide a basis for understanding and insights into the molecular mechanism of thrombus maturation.

METHODS

Data and Materials Availability

RNA-seq data of the thrombi were deposited in the National Institutes of Health Gene Expression Omnibus with accession ID PRJNA1099305 and can be accessed by https://www.ncbi.nlm.nih.gov/sra/PRJNA1099305. The clinical data are available upon request from the corresponding author.

Sample Collection and Total RNA Isolation

This study was approved by the Ethics Committees of the Toyonaka Municipal Hospital in accordance with the Declaration of Helsinki, and all participants provided written informed consent before commencement of the study. The clinical backgrounds of the participants are shown in Table S1. Thrombi retrieved from 5 patients with acute ischemic stroke were stored in RNAlater (Thermo Fisher, Waltham, MA) overnight at 4 °C promptly after mechanical thrombectomy. The thrombi were then transferred to a −80°C freezer until subsequent analyses. Whole blood was sampled from the

patients via the femoral arterial sheath during the mechanical thrombectomy and stored using a PAXgene RNA blood collection tube (762 165; BD Biosciences, San Jose, CA) in a −80 °C freezer until subsequent steps. Total RNA was extracted from each thrombus using a ReliaPrep RNA tissue MiniPrep System (Z6110; Promega, Madison, WI) and from whole blood using a PAXgene Blood RNA Kit (762 164; Qiagen, Hilden, Germany), according to the respective manufacturers' instructions.

Library Preparation and Sequencing

The purity and quantity of the isolated total RNA were assessed using a NanoDrop 2000 spectrophotometer (Thermo Fisher). The RNA integrity number (RIN) was assessed using a Bioanalyzer 2100 system (Agilent, Santa Clara, CA). The 3 thrombus RNA samples with the highest RINs and their paired blood RNA samples were subjected to subsequent analyses. The RINs for the thrombus samples were 8.0, 6.8, and 4.5, and those for the paired blood samples were 7.2, 7.1, and 7.7. Total RNA samples were subjected to library preparation using the Illumina TruSeq Stranded Total RNA Library Prep Kit with Ribo-Zero Globin (Illumina, San Diego, CA), according to the manufacturer's protocol. RNA libraries were subjected to 100-bp paired-end sequencing on a NovaSeq 6000 system (Illumina) with a median of 40 million reads.

RNA-Seq Data Processing, Mapping, and Counting

Sequence quality was assessed using FastQC (version 0.12.1, Babraham Bioinformatics), and reads were trimmed using Trimmomatic (version 0.36).[20] The reads were mapped to GRCh38 using HISAT2 software (version 2.2.1).[21] Mapped reads were counted using the feature Counts (version 2.0.3).[22] All these procedures were performed on the Galaxy platform,[23] and default parameters were used.

Differentially Expressed Genes and Enrichment Analysis

Differentially expressed genes (DEGs) between the thrombi and blood were identified using an integrated browser application, iDEP1.1.[24] Minimal counts of 1.5 per million in at least 2 libraries were set in the preprocessing data interface, and the count data were subjected to a variance-stabilizing transformation for clustering. A heat map was generated to include the top 2000 genes. Unsupervised hierarchical clustering was performed using 1-Pearson correlation and average linkage. DEGs were identified using the iDEP built-in DESeq2 package[25] with a threshold of false discovery rate <0.01 and a minimum absolute value of fold change >4.

Enrichment analysis was performed using the DEGs defined above to determine the most enriched gene ontology pathways in terms of biological processes, cellular components, and molecular functions. Genes with a false discovery rate >0.6 were removed from the pathway analysis. The top 20 pathways were displayed as a network. Nodes were connected if they shared ≥20% genes. All parameters not specified above were left as the default values. Pathway clusters were manually annotated.

Protein–Protein Interaction Analysis

The protein–protein interactions between all DEGs upregulated in the thrombus, except for mitochondrial genes, were analyzed using the Search Tool for the Retrieval of Interacting Genes database (version 12.0).[26] A minimal interaction score of 0.4 was set as the default. Hub genes were identified using Cytoscape (version 3.10.1) software and the CytoHubba plugin (version 0.1).[27] DEGs with the highest Matthews correlation coefficient scores were considered hub genes. The DEGs were clustered using Markov clustering with a default inflation parameter of 3. Gene ontology enrichment analysis was performed on these clusters. Clusters were manually annotated on the basis of the enriched pathways and visualized using Cytoscape software.

Deconvolution of the Bulk RNA-Sequencing Data

Bulk RNA-sequencing data were deconvoluted using scRNA-seq data from peripheral leukocytes of healthy adults, applying the MuSiC package (version 1.0.0) with default parameters.[28] The scRNA-seq data were obtained from a public database (GSE216009).[29]

Quantitative Polymerase Chain Reaction Analysis

Reverse transcription–quantitative polymerase chain reaction was performed to amplify and detect *SPP1* from 5 pairs of thrombus and blood RNA samples, comprising 3 pairs used for RNA-seq analysis and 2 additional pairs. First, cDNA was prepared by reverse-transcribing 400 pg of total RNA using Superscript III and random primers (Thermo Fisher Scientific). The resulting cDNA was used for real-time PCR analysis using a Platinum SYBR Green quantitative polymerase chain reaction SuperMix (Thermo Fisher Scientific). Next, 100 reverse transcription products and standard plasmids were subjected to real-time polymerase chain reaction analysis (QuantStudio 7 Flex Real-Time PCR System; Applied Biosystems) using human β-actin as an internal

control. The following polymerase chain reaction program was used: 10 minutes of denaturation at 95 °C, and then 40 cycles of 95 °C for 15 seconds, 58 °C for 30 seconds, and 72 °C for 30 seconds. The primers used are listed in Table S2.

Histological Analysis of the Thrombus

We examined 168 consecutive patients who underwent mechanical thrombectomy for acute ischemic stroke between January 2015 and December 2019 at 2 tertiary referral hospitals with comprehensive stroke centers in Japan (Osaka University Hospital, Osaka; Osaka General Medical Center, Osaka). Thrombus specimens were available for 76 patients. Patients with left ventricular assist devices, atherosclerotic intracranial stenosis, or cerebral artery dissection were excluded. Finally, 66 patients with thrombi retrieved during mechanical thrombectomy for cerebral embolisms were included in this study (Figure S1). Clinical data were also collected from the included patients. The detailed methods for clinical data collection were performed as previously described.[17]

Immunohistochemistry Staining and Histological Analysis

Thrombus samples were fixed in 10% neutral-buffered formalin and embedded in paraffin. To identify the presence of osteopontin, a product of *SPP1*, 3 primary antibodies were used: mouse monoclonal antibodies (10011, 1:200; IBL, Gunma, Japan), rabbit polyclonal antibodies (25715-1-AP, 1:800; Proteintech, Rosemont, IL), and rabbit polyclonal antibodies against the N-terminal region of human osteopontin (18625, 1:200; IBL). We used human gallbladder and kidney samples as positive controls in staining to determine the optimal antibody concentrations. COL6 was detected using rabbit polyclonal anti-COL6 antibody (ab182744, 1:800; abcam, Cambridge, UK). IHC staining was performed using a Roche Ventana BenchMark GX autostainer (Ventana Medical Systems, Tucson, AZ), according to the manufacturer's instructions. The stained slides were captured as digital images using a VS200 Slide Scanner (Olympus, Tokyo, Japan). COL6 expression was semi-quantified in the following manner: 0, not detected; 1, observed only in 1 part; 2, observed in >2 parts; and 3, observed in the inner part of the specimen. The age, size, and components of the thrombi and the extent of activation and release of neutrophil extracellular traps were evaluated as previously described.[17] Thrombus age was evaluated based on hematoxylin and eosin staining and positivity for anti–α-smooth muscle actin (M0851, 1:800; Agilent Technologies, Santa Clara, CA).[30] Thrombus size and red blood cell proportion were measured using hematoxylin and eosin staining; fibrin was detected using phosphotungstic acid–hematoxylin staining; and platelets were subjected to immunohistochemistry staining to assess CD42b (sc-80728, 1:200; Santa Cruz Biotechnology, Dallas, TX). The density of monocytes and macrophages was determined through staining for CD163 (NCL-L-CD163, 1:100; Leica Biosystems, Wetzlar, Germany), and the extent of activation and release of neutrophil extracellular traps was determined using H3Cit staining (ab5103, 1:3200; Abcam, Cambridge, UK). Representative images of these staining have been published previously.[17] Anti–plasminogen activator inhibitor-1 (PAI-1) antibody (ab66705, 1:400, Abcam) was used to detect PAI-1–positive cells in the thrombi. A thrombus was considered osteopontin-high when the aggregation of osteopontin-positive cells was observed. In addition, 4 samples were subjected to double staining with anti-osteopontin and anti–neutrophil elastase antibodies or with anti-osteopontin and anti-CD163 antibodies.

scRNA-Seq Data Analysis of CTEPH Thrombi

Publicly available scRNA-seq data of thrombi collected from patients with CTEPH, which were deposited by Viswanathan et al (PRJNA929967), were obtained.[31] Filtered matrices were loaded into the R package Seurat (version 5.0; R Foundation for Statistical Computing, Vienna, Austria),[32] and cells with <200 features, >9000 features, <300 Unique Molecular Identifiers, >60000 Unique Molecular Identifiers, or >15% mitochondrial gene fractions were removed. Normalization was performed using the R package sctransform,[33] followed by the integration workflow of Seurat. Principal component analysis was performed on the integrated data, and the top 30 principal components were used to cluster the cells. The FindNeighbors and FindClusters functions in Seurat were used to identify cell clusters with a resolution of 1.0. The FindAllMarkers function in Seurat was used to identify the markers for each cluster. Clusters were manually annotated using known lineage markers and several clusters were combined as necessary. Monocytes and macrophages were defined as cells with a high *CD14* or *CD163* expression. monocytes and macrophages were subjected to subclustering using a resolution of 0.2. DEGs from each subcluster were calculated using the FindAllMarkers function, and the top 10 upregulated genes were used for the DoHeatmap function.

Pathway enrichment analysis was performed using the enrichGO function in the R package clusterProfiler.[34] We set the adjusting P method to false discovery rate, the threshold to 0.05, the minimum gene set size to 10, and the maximum gene set size to 600. Pathways that included <3 genes were excluded. The top 40 pathways with the smallest *P* values were visualized using the Emapplot function, and the bound pathways were automatically clustered using the Emapplot function.

The ligand–receptor interaction between each subcluster of monocytes and macrophages and fibroblasts was analyzed using CellChat (version 2.1).[35] Normalized data were used for each condition, and cell types with <10 cells were excluded. Interaction strength refers to the probability of communication between a given ligand and receptor. It was calculated as the degree of cooperativity and interactions derived from the law of mass action and the degree to which the ligands and receptors are expressed.

scRNA-Seq Data Analysis of Cells from Murine Venous Walls

We obtained scRNA-seq data from cells of the vein wall of a mouse DVT model, which were deposited by DeRoo et al (PRJNA916965).[36] They harvested the vessel wall from the inferior vena cava 24 hours after ligation. Sham surgery involved vessel dissection without interruption. Cells with <800 features, >8000 features, <1000 Unique Molecular Identifiers, >40000 Unique Molecular Identifiers, or >20% mitochondrial gene fractions were removed from the analysis. Data analysis was performed as described above, except that the top 15 principal components were used and that clustering was performed with a resolution of 0.2. Identified monocytes and macrophages were subjected to subclustering using the top 15 principal components and a resolution of 0.6.

Statistical Analysis

Continuous variables were reported as the median and interquartile range, whereas categorical variables were reported as numbers and percentages. Continuous variables were compared using the Wilcoxon rank-sum test. Categorical variables were compared using Fisher's exact test. The cumulative rate of successful reperfusion was evaluated using the Kaplan–Meier method. The association between osteopontin and COL6 expressions, and the association between the COL6 expression number of passes were tested using ordinal logistic regression. It was confirmed that the proportional odds assumption was met using the score test provided by PROC LOGISTIC in SAS (SAS Institute Inc., Cary, NC). Statistical significance was set at $P<0.05$. All analyses were performed using SAS Studio software (version 9.4; SAS Institute Inc.).

RESULTS

RNA Expression in Thrombi Differs From That in Blood

Mechanical thrombectomy is an endovascular surgery procedure that has rapidly developed over the past decade to recanalize occluded cerebral vessels in patients with acute ischemic stroke. In the present study, we compared the RNA expression profile in 3 thrombi retrieved from cerebral vessels through mechanical thrombectomy with that of simultaneously sampled blood as a substitute for a newly formed thrombus (Figure 1A). All patients were diagnosed with a cardiogenic embolism (Table S1). The heatmap in Figure 1B shows a substantial difference in RNA expression between the thrombus and blood. Unbiased clustering detected sample differences (Figure 1C). Compared with that in the blood, a total of 1121 genes were significantly upregulated and 693 were downregulated in the thrombus (Figure 1D). The top 20 upregulated DEGs included proinflammatory chemokines such as *CXCL8* and *CCL2*, consistent with a previous report (Figure 1E).[37] Genes related to the ECM, such as *FN1* and *SPP1*, were noted to be upregulated in the thrombi.

Gene Sets Related to ECM Were Enriched in Thrombi

The results of the enrichment analysis are shown in Figure 2A as network plots. Biological process analysis revealed clusters, including tissue morphogenesis and ECM organization. Cellular component analysis revealed clusters of ECM, cell adhesion, and mitochondrial components. Molecular function analysis revealed clusters of chemokine activity, cell adhesion, and ECM constituents. All analyses showed that pathways related to the ECM were significantly enriched. Genes related to ECM were highly expressed in thrombi (Figure S2).

Protein–Protein Interaction Analysis Identified SPP1 as a Hub Gene

Among the 1121 upregulated DEGs, 1038 genes were identified in the Search Tool for the Retrieval of Interacting Genes database after excluding the mitochondrial genes. We then identified 23 hub genes using CytoHubba (Figure S3). Unbiased Markov clustering identified 278 clusters using 963 genes. The top 4 clusters, which included the most genes among the identified clusters, are visualized in Figure 2B. Cluster 1 included 55 genes associated with ECM formation; cluster 2 included 31 genes related to the anti-inflammatory response; cluster 3 included 26 genes related to the ERBB signaling pathway, and cluster 4 included 25 genes related to proinflammatory cytokines. Fifteen hub genes were included in the top 4 clusters.

We identified 5 hub genes (*FN1*, *MMP2*, *IGF1*, *SERPINE1*, and *SPP1*) in the ECM formation cluster, as this cluster included the most genes and pathways related to ECM that were highly enriched in the enrichment analysis (Figure 2A). *FN1* encodes for fibronectin, a

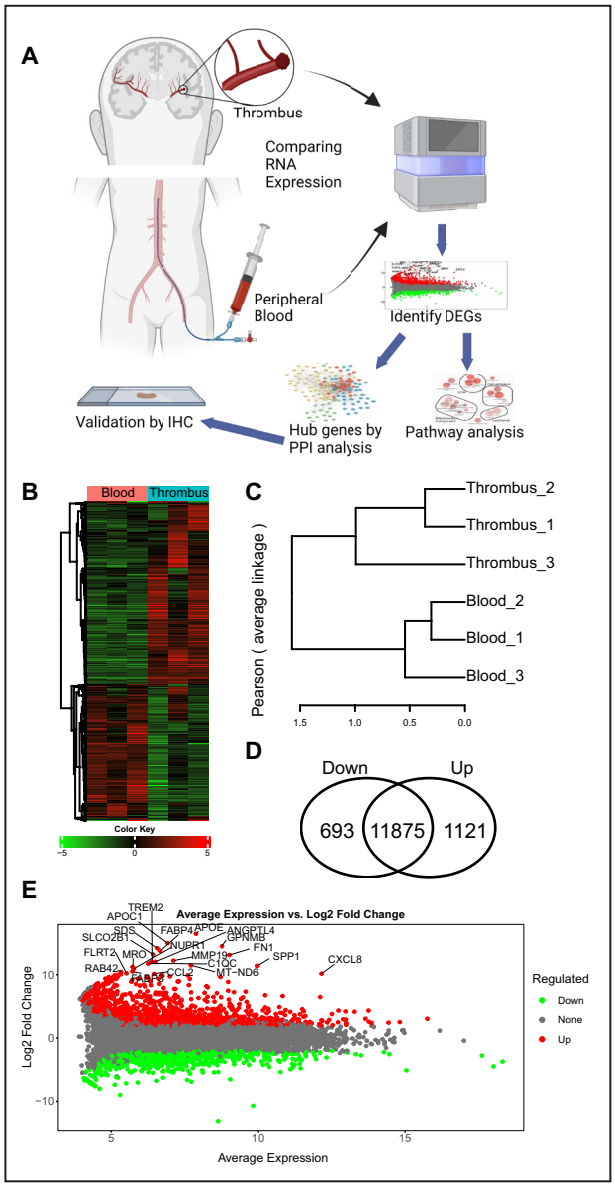

Figure 1. Comparison of gene expression profiles between the thrombi and blood.

A, Summary of the analytical results. **B**, Heatmaps of the gene expression patterns. **C**, Unsupervised hierarchical clustering of the samples. **D**, Number of upregulated and downregulated genes in the thrombi compared with that in the blood. **E**, MA plot of the genes. Genes upregulated in thrombi are shown in red, and genes with the top 20 highest fold changes are annotated. DEGs indicates differentially expressed genes; IHC, immunohistochemistry; and PPI, protein–protein interaction.

glycoprotein involved in cell adhesion, migration, wound healing, and embryonic development. Fibronectin is vital for bleeding control.[38] *MMP2* encodes matrix metalloproteinase-2, which is involved in the degradation and remodeling of various ECM components. *MMP2* inactivation prevents thrombosis and prolonged bleeding time.[39] Insulin-like growth factor 1 (IGF-1) is essential in the insulin signaling pathway and is a key growth factor involved in various processes such as cell proliferation, maturation, differentiation, and survival.[40] It also regulates fibroblast growth and ECM deposition.[41] *SERPINE1* encodes PAI-1; its deficiency causes abnormal bleeding.[42] *SPP1* encodes osteopontin, a secreted multifunctional glycophosphoprotein that plays an important role in physiological and pathophysiological processes.[43] Osteopontin drives immune responses under ischemic conditions and induces neutrophil and macrophage infiltration.[44–46] It was recently reported that osteopontin is a ligand for integrin α9β1, a potential target for preventing arterial thrombosis.[47–49] Therefore, we decided to investigate whether osteopontin is present in thrombi retrieved from cerebral vessels and to determine how osteopontin is associated with the clinical characteristics of patients who underwent mechanical thrombectomy.

To confirm that the elevation of *SPP1* expression in thrombi was not due to changes in the proportion of cell types, we deconvoluted the bulk RNA sequencing data. The proportions of monocytes and platelets were higher in thrombi (Figure S4A). *SPP1* expression remained elevated in thrombi even after normalization to the proportion of monocytes (Figure S4B).

As a sensitivity analysis, we repeated the same analysis after excluding the thrombus sample with the lowest RIN. The most significantly upregulated genes remained largely consistent with those identified in the original analysis (Figure S5A). Enrichment analysis similarly revealed upregulation of pathways related to the ECM in thrombi, consistent with the original analysis (Figure S5B).

Osteopontin Is Expressed by Monocytes and Macrophages in Thrombi

We first validated *SPP1* expression using reverse transcription-quantitative polymerase chain reaction with 5 pairs of samples, adding 2 other pairs to the samples used for RNA sequencing. In the thrombi retrieved from the cerebral artery, *SPP1* expression was elevated compared with that in the blood (Figure 3A). In addition, the expression of *TIMP1*, which is modulated by osteopontin and related to ECM,[50] was also elevated.

Next, we performed immunohistochemistry staining of paraffin-embedded thrombus samples using 3 anti-osteopontin antibodies. All antibodies validated the presence of osteopontin in thrombi (Figure S6). All the observed samples were positive for osteopontin, but the extent varied (Figure 3B and 3C). Heterogeneous osteopontin positivity was observed in many thrombi; within individual thrombi, some regions exhibited strong staining, whereas others were negative, as exemplified by the thrombus shown in Figure 3D. Osteopontin-positive

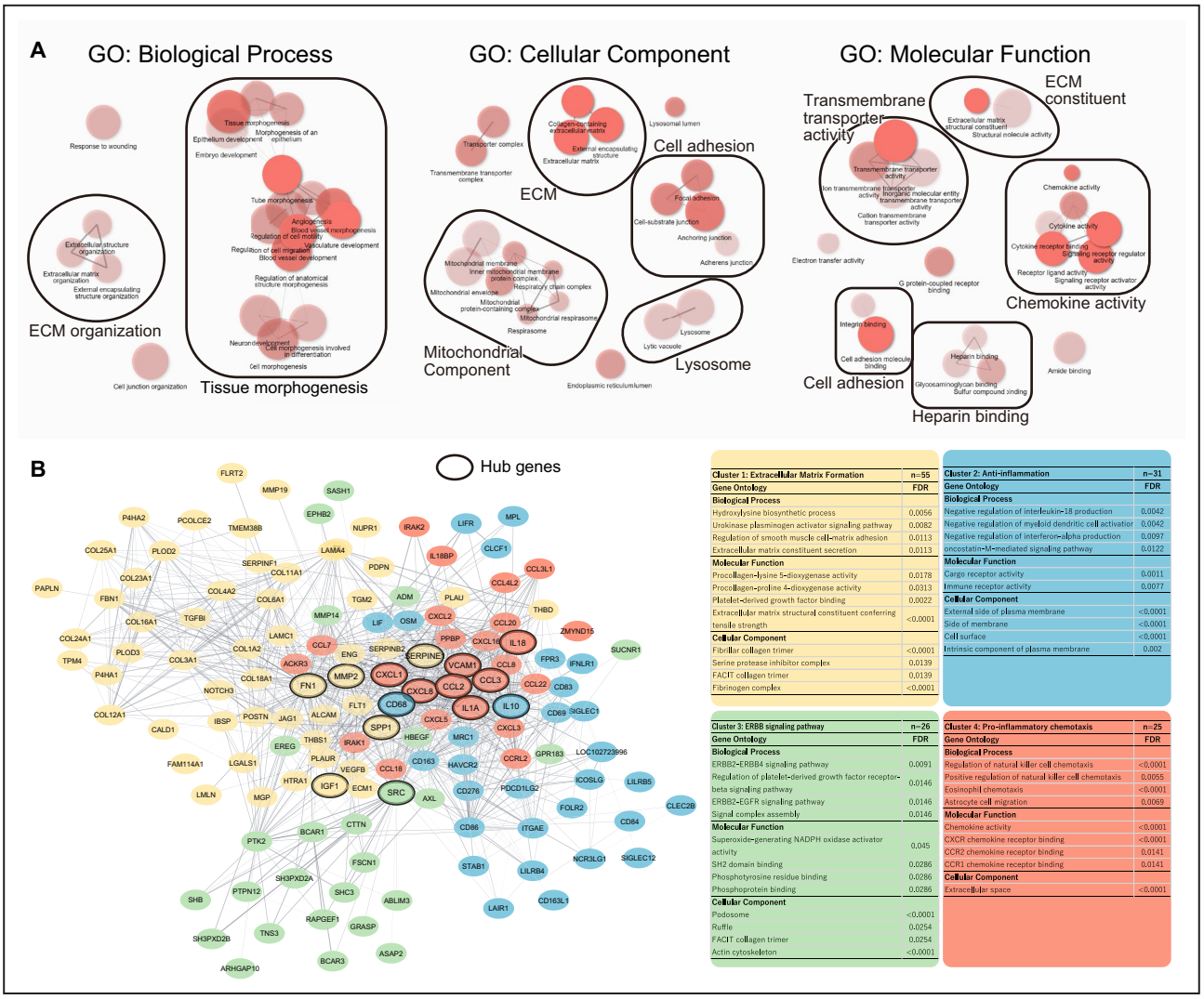

Figure 2. Enrichment and PPI analysis.
A, Enrichment analysis results. The top 20 upregulated pathways in each category are visualized. Pathways sharing genes are connected by edges. The width of the edges represents the number of shared genes. The pathways were manually clustered and annotated. **B**, PPI network. Genes belonging to the top 4 clusters of the 963 upregulated genes identified in the Search Tool for the Retrieval of Interacting Genes database are visualized. Clustering was performed using Markov clustering, and each cluster is represented by a different color. The thickness of each edge represents the level of confidence. Hub genes are identified through their Matthews correlation coefficients and are indicated with bold circles. Enrichment analysis results based on each cluster are shown as a table on the right and are arranged based on strength. Cluster annotation was performed manually. FDR indicates false discovery rate; and PPI, protein–protein interaction.

cell aggregation (where osteopontin-positive cells were observed as a cluster) was also observed when the thrombus was strongly positive for osteopontin. Thus, we classified the thrombi into osteopontin-high or osteopontin-low according to the presence or absence of osteopontin-positive cell aggregation. Double staining revealed that osteopontin was not expressed by neutrophils that are defined as cells with a lobulated nucleus and positive for neutrophil elastase (Figure 3E). Osteopontin was primarily expressed by monocytes and macrophages in the thrombi (Figure 3F).

Osteopontin Expression Correlates to COL6 Expression in Stroke Thrombi

Next, we examined whether osteopontin expression correlates to ECM formation in the thrombi. For this, we reviewed the collagen gene expressions in the RNA-seq data and determined that *COL6A1* and *COL7A1* were expressed in thrombi (Figure 4A). As COL6 is expressed by fibroblast in the wound healing and regulates dermal matrix assembly,[51,52] we decided to investigate the association between osteopontin and COL6 expression. We analyzed 66 thrombi retrieved

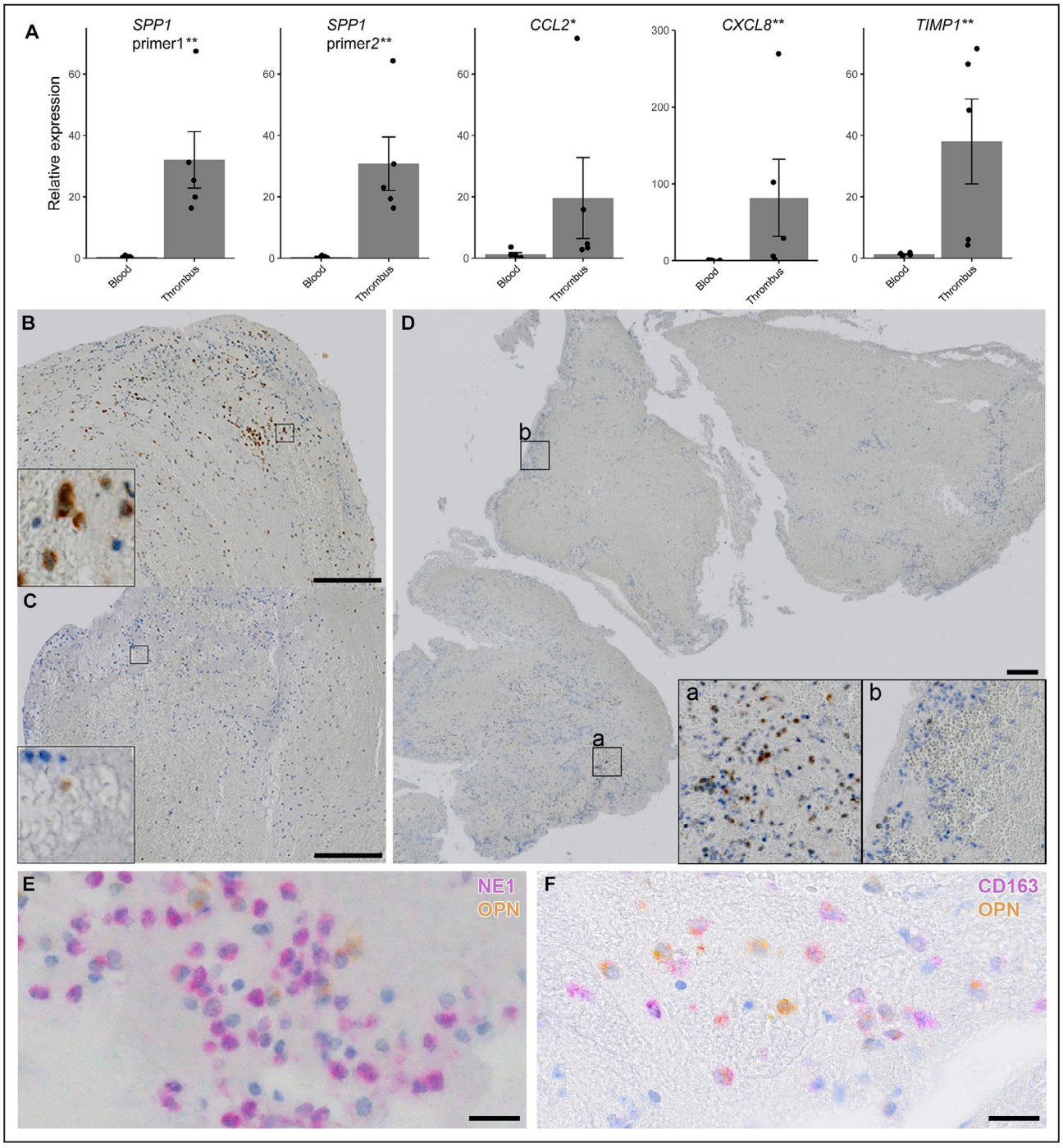

Figure 3. Immunohistochemical staining shows the presence of osteopontin in thrombi.
A, Gene expression as measured using quantitative polymerase chain reaction. **B** through **D**, Immunohistochemical staining for osteopontin using rabbit polyclonal antibodies against the N-terminal part of human osteopontin (18625). Boxed areas are magnified in the panel. Bar=200 μm. **B**, Representative image of a thrombus with strong positivity for osteopontin. Aggregation of osteopontin+ cells was observed. **C**, Thrombus with weak positivity for osteopontin. D, Osteopontin-positive cells unevenly distributed in 1 thrombus. **E**, Double-staining against neutrophil elastase 1 (purple) and osteopontin (yellow). Bar=20 μm (**F**) Double-staining against CD163 (purple) and osteopontin (yellow). OPN indicates osteopontin.

during mechanical thrombectomy for cerebral embolisms (Figure S1). Among the 66 samples, 40 were osteopontin-high and 26 were osteopontin-low. COL6 expression was mostly observed only on the surface of the thrombus (Figure 4B). Semiquantification of the COL6 expression showed a positive correlation between osteopontin and COL6 expression in thrombi (P<0.001; Figure 4C).

Effect of COL6 Expression on Resistance to Thrombectomy

Following the identification of COL6 in thrombi, we examined whether this ECM formation is of clinical significance. When a thrombus is resistant to thrombectomy, the number of passes required for reperfusion and the time from puncture to reperfusion are increased. Thus, we compared the time to reperfusion across the presence of COL6 in thrombi in the 66 patients using time to event analysis. The presence of COL6 was marginally associated with longer time to reperfusion (log-rank P=0.090; Figure 5A) and more passes (P=0.110; Figure 5B).

Osteopontin Expression and Thrombus Features

Next, we explored the characteristics of thrombi with high osteopontin expression. First, we compared the features of the thrombi on the basis of osteopontin expression. Fresh thrombi were less common among osteopontin-high samples (2.5% versus 46.2%, P<0.001; Figure S7A). No significant differences were observed in the proportions of red blood cells, fibrin, or platelets. The density of monocytes and macrophages was higher in the osteopontin-high samples (Figure S7B). PAI-1–positive cells tended to be more frequent in osteopontin-high thrombi than in osteopontin-low thrombi (40.0% versus 15.4%, P=0.054; Figure S7C).

Osteopontin Expression and Clinical Characteristics

We also investigated the differences in clinical characteristics by comparing patient backgrounds according to osteopontin expression (Table S3). The proportion of patients with atrial fibrillation was marginally higher (54% versus 78%, P=0.060), the level of brain natriuretic peptide was marginally higher (82.5 versus 225 pg/mL, P=0.054), and the cardiothoracic ratio was significantly higher (57% versus 62%, P=0.023) in patients with osteopontin-high thrombi. The proportion of stroke subtypes also differed significantly across osteopontin expression (P=0.043; Figure S8); the proportion of cardioembolic stroke was higher among patients with osteopontin-high thrombi.

SPP1-High Monocytes and Macrophages in Thrombi Are Related to ECM Formation

Thus far, we have shown the potential importance of *SPP1* expression in ECM formation in stroke thrombi. However, these observations cannot be applied to chronic thrombi such as deep venous thrombi, because stroke thrombi are mostly <5 days old.[17,19] In addition, the molecular mechanism how *SPP1*-positive monocytes and macrophages promote ECM formation remains unclear. To assess these questions, we used scRNA-seq data of thrombi from patients with CTEPH.[31] After unbiased clustering (Figure S9), we successfully identified monocytes and macrophages (Figure 6A and 6B). Fibroblasts in these CTEPH thrombi expressed *COL1A1* and *COL3A1*, not only *COL6A1* (Figure 6B), consistent with the supposition that these thrombi were older than stroke thrombi. *SPP1* was also primarily expressed by monocytes and macrophages in these samples. Four subclusters of monocytes and macrophages were identified (Figure 6C), and *SPP1* was listed as one of the top 10 highly expressed genes in subcluster 2 (Figure 6D). Hub gene expressions identified through protein–protein interaction analysis are shown in Figure 6E. *CD68* was highly expressed in subcluster 2, whereas *CXCL8* and *CCL3* were highly expressed in subcluster 1. Enrichment analysis revealed that pathways related to the ECM were upregulated in subcluster 2 (Figure 6F, red circle). Pathways related to lysosomes (Figure 6F, pink and light blue circles) were also upregulated in subcluster 2, indicating the possible involvement of this subcluster in the formation and remodeling of ECM. In addition, pathways related to inflammation, such as the cellular response to tumor necrosis factor, response to interleukin-1, and chemotaxis, were enriched in subcluster 1 (Figure S10A).

To further understand the role of subcluster 2 (*SPP1*-high monocytes and macrophages) in thrombus formation, we performed a ligand-receptor interaction analysis using CellChat. Dense communication between monocytes and macrophages and fibroblasts, which are the major source of ECM, was inferred in the thrombi from patients with CTEPH (Figure 7A). Among the immune cells found in the thrombus, monocytes and macrophages in subcluster 2 showed the highest number and strength of inferred ligand-receptor interactions as the sender between fibroblasts (Figure 7B). When monocytes and macrophages were assigned to the sender, the ligand–receptor pairs *SPP1-ITGAV_ITGB1*, *SPP1-ITGA8_ITGB1*, and *SPP1-ITGAV_ITGB5* were inferred to be the primary communicators between subcluster 2 monocytes and macrophages and fibroblasts (Figure 7C and 7D). In addition, ligand–receptor pairs of *PDGFB-PDGFRB* were inferred between subcluster 1 monocytes and macrophages and fibroblasts (Figure S10B).

SPP1-High Monocytes and Macrophages Are Expanded in Murine Venous Vessel Walls After Thrombosis Induction

As monocytes and macrophages are presumed to migrate into the thrombus through the vessel wall,[53]

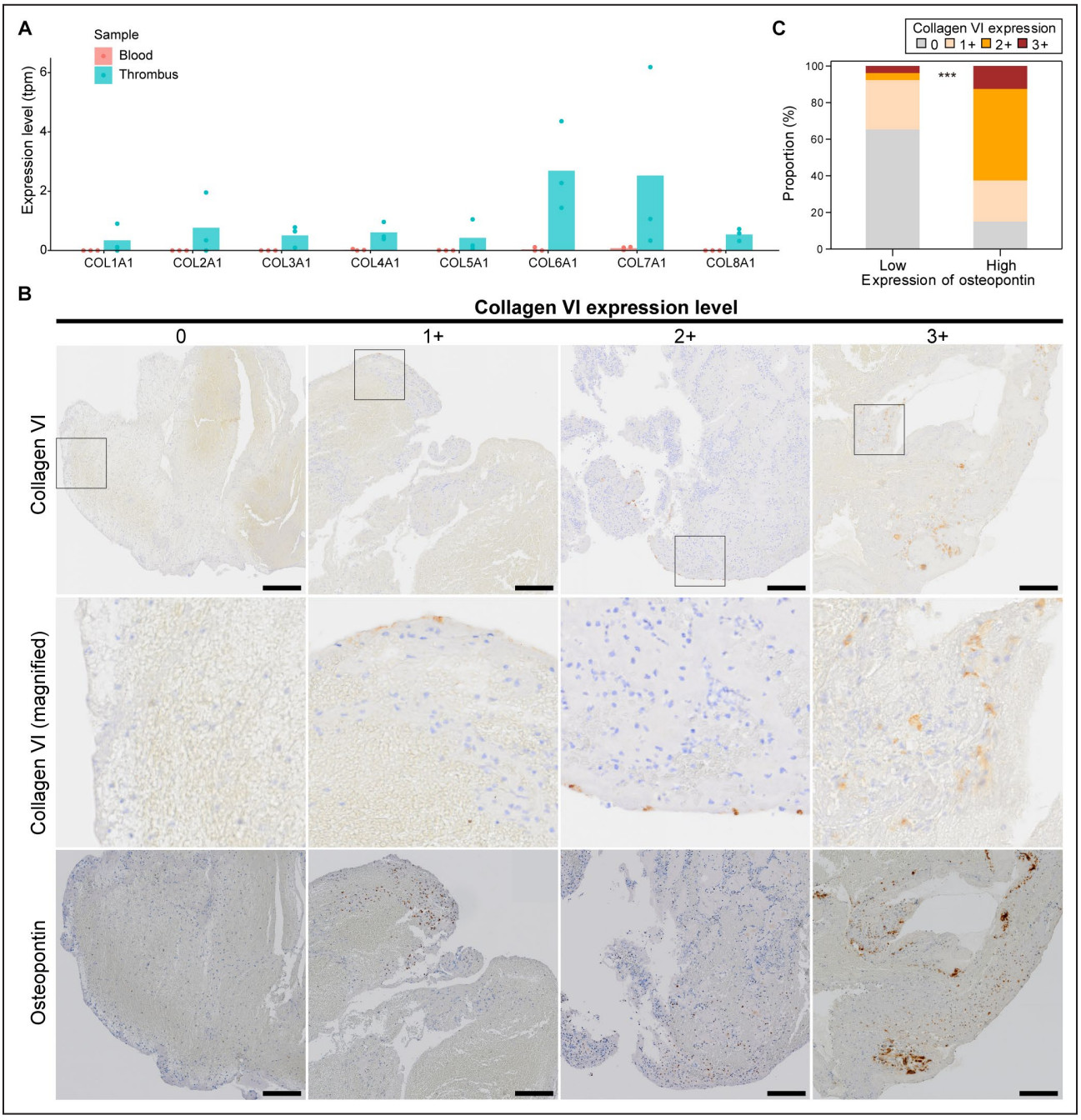

Figure 4. Osteopontin expression correlates to COL6 expression in stroke thrombi.
A, Collagen mRNA expression measured as transcripts per million (tpm) in blood and thrombi. **B**, Immunohistochemical staining for osteopontin and COL6. COL6 expression was semiquantified. Boxed areas are magnified in the panel. Bar=200 μm. **C**, Association between osteopontin and COL6 expressions. *P<0.05, **P<0.01, and ***P<0.001. COL6 indicates collagen type VI.

we hypothesized that *SPP1*-high monocytes and macrophages may be present in the vessel wall after thrombosis. We investigated *SPP1* expression through monocytes and macrophages in the venous vessel walls of mice with and without deep vein thrombosis (Figure S11A–D). Our results showed that the subcluster of monocytes and macrophages with high *SPP1* expression was expanded in the deep vein thrombosis group (Figure S11E).

DISCUSSION

Thrombus age has recently been reconsidered as a critical factor influencing resistance to reperfusion therapy

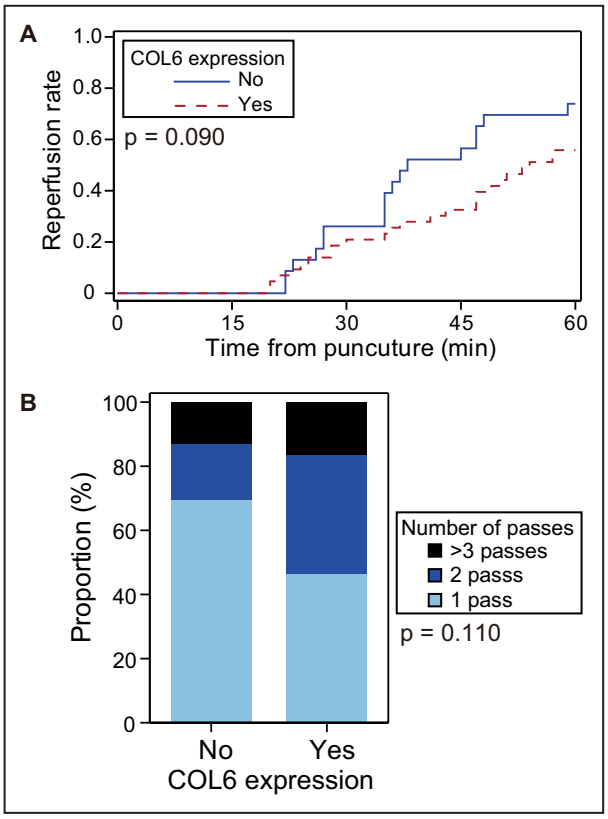

Figure 5. Association between resistance to thrombectomy and COL6 expression in the thrombus.
A, Cumulative rate of successful reperfusion (expanded treatment in cerebral ischemia ≥2b) after puncture. **B**, Proportion of the number of passes before successful reperfusion. COL6 indicates collagen type VI.

in cerebral embolism.[17–19,54] Although it is well known that a thrombus matures as time passes and that its component and physical features dynamically change after formation,[14–16] the detailed process of thrombus maturation in embolism is not yet well understood. In the present study, we aimed to clarify the molecular basis of thrombus maturation using comprehensive bioinformatics analysis and immunohistochemistry of the thrombi of patients. We elucidated the transcriptional landscape after thrombus formation by comparing RNA expression in thrombi from acute cerebral infarctions with that in simultaneously collected peripheral blood. In addition to proinflammatory responses, which have been reported previously,[37] our findings revealed an anti-inflammatory response and ECM formation in thrombi. *SPP1* was upregulated and was identified as a hub gene of ECM formation in thrombi. Immunohistochemistry analysis showed that the expression of *SPP1* translation product, osteopontin, correlated to COL6 expression in thrombi. This correlation does not guarantee the causal relationship between *SPP1* expression and ECM formation in thrombi; however, considering the increased CCI between *SPP1*-high monocytes and macrophages and fibroblasts shown in the scRNA-seq and given a number of reports, which demonstrate the involvement of *SPP1*-positive macrophages in tissue fibrosis,[55–60] *SPP1*-high monocytes and macrophages in thrombi likely contributed to ECM formation. Collectively, our findings indicate that *SPP1*-high monocytes and macrophages play a key role in thrombus maturation, which may contribute to resistance to reperfusion therapy.

SPP1-positive macrophages have recently been identified as key cell types promoting tissue fibrosis.[55–60] In line with these reports, the results of enrichment analysis indicate that subcluster 2 monocytes and macrophages (*SPP1*-high) are related to the ECM in the thrombi of patients with CTEPH. This was supported by the results of our ligand-receptor interaction analysis. Integrin αV, an osteopontin receptor expressed by fibroblasts, plays key roles in fibrotic diseases.[61,62] The interaction between osteopontin and integrins αVβ1 and αVβ5 has been reported to contribute to the adhesion of smooth muscle and fibroadipogenic progenitor cells[58,63]; osteopontin is also chemotactic for smooth muscle cells.[64] Thus, *SPP1*-high monocytes and macrophages may promote ECM formation by recruiting fibroblasts to the thrombus. Nonetheless, our results do not exclude the possibility that other subclusters of monocytes and macrophages are involved in ECM formation in the thrombus. Subcluster 1 monocytes and macrophages have been shown to promote fibrogenesis through *PDGFB-PDGFRB* interactions. In addition, the *THBS1–CD47* interaction, which has been reported to promote fibrosis,[65] was also observed in other subclusters. Further investigations are required to clarify the role of heterogeneous monocytes and macrophages in ECM formation in thrombi.

Osteopontin-positive cells were not evenly distributed throughout the thrombus in thrombi retrieved from cerebral vessels. They were often densely aggregated in certain areas, particularly around the periphery of the thrombus. These aggregations of osteopontin-positive cells are presumed to occur sometime after thrombus formation, as they are less common in fresh thrombi. In deep vein thrombosis, macrophages are presumed to increase migrating from the vascular wall to the thrombus during venous thrombosis.[17,53,66] The present study showed that *SPP1*-high monocytes and macrophages were expanded in the venous wall after thrombosis induction. Moreover, a recent study revealed that *SPP1*-positive macrophages are expanded in the left atrial tissue of patients with persistent atrial fibrillation and can serve as targets for immunotherapy in atrial fibrillation.[60] Therefore, some of the osteopontin-positive monocytes and macrophages observed in thrombi from patients with cardioembolic stroke may have migrated from the left atrial wall. The observation in the present study that patients without atrial fibrillation had

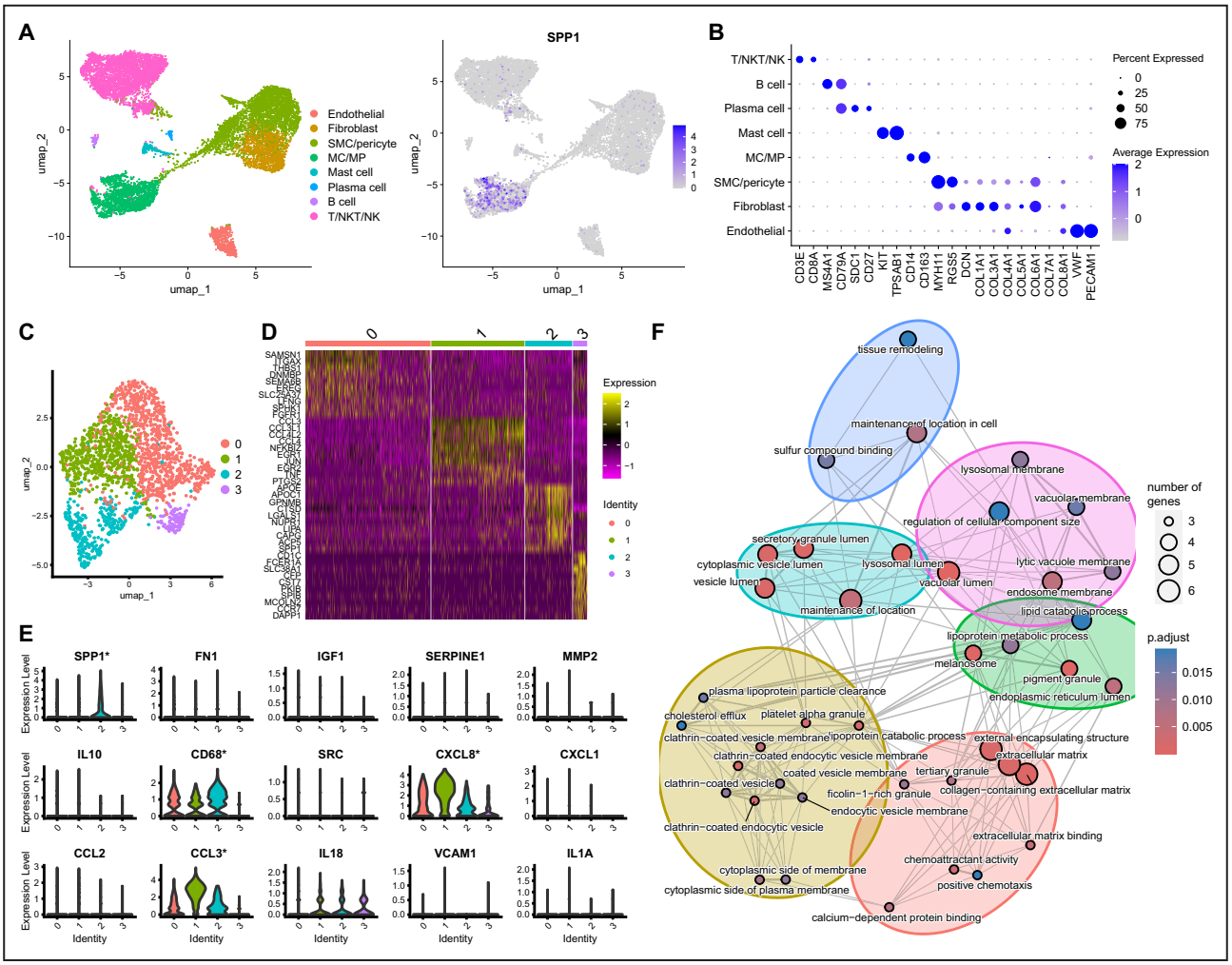

Figure 6. Analysis of scRNA-seq data of thrombi from patients with chronic thromboembolic pulmonary hypertension. (**A**) UMAP plot illustrating cell type and feature plot of *SPP1* expression. **B**, Expression of specific marker and collagen genes. *COL2* genes were not detected in these data. **C**, Subclustering of the monocytes and macrophages. Four subclusters are identified. **D,** Heatmap of the top 10 DEGs based on each subcluster of monocytes and macrophages. *SPP1* is highly expressed in subcluster 2. **E**, Hub gene expressions determined through PPI analysis in the thrombus. **P*_val_adj<0.0001. (**F**) Enrichment analysis results. Pathways upregulated in subcluster 2 monocytes and macrophages are visualized. Pathways sharing genes are connected by edges, and the width of the edges represents the number of shared genes. Clustering was performed automatically. DEG indicates differentially expressed gene; PPI, protein–protein interaction; scRNA-seq, single-cell RNA sequencing; and UMAP, uniform manifold approximation and projection.

fewer osteopontin-high thrombi supports this hypothesis. Therefore, the migration of osteopontin-positive monocytes and macrophages may be a potential target for novel antithrombotic therapies.

More monocytes and macrophages were observed in osteopontin-high thrombi than in osteopontin-low thrombi. Additionally, although not statistically significant, a greater number of PAI-1–positive cells was found in osteopontin-high thrombi. Osteopontin is known to recruit macrophages and fibroblasts; therefore, its expression in thrombi may promote the infiltration of PAI-1–secreting cells, potentially contributing to resistance to fibrinolysis. Since the density of monocytes and macrophages is higher in older thrombi than in fresh ones[17,67] and the number of PAI-1–positive cells increases over time, these associations may suggest that osteopontin-high thrombi are generally older than osteopontin-low thrombi.

Intracardiac thrombi are frequently encountered in clinical practice, and the prevalence of left atrial appendage thrombus formation has been estimated to range from 5% to 27% in patients who have not previously received anticoagulant therapy.[68] Patients with intracardiac thrombi are at an elevated risk of developing cardiogenic embolisms. Thus, convenient and cost-effective screening methods for intracardiac thrombi are required. In a recent study, osteopontin has been recognized as a biomarker for vascular diseases.[43] The

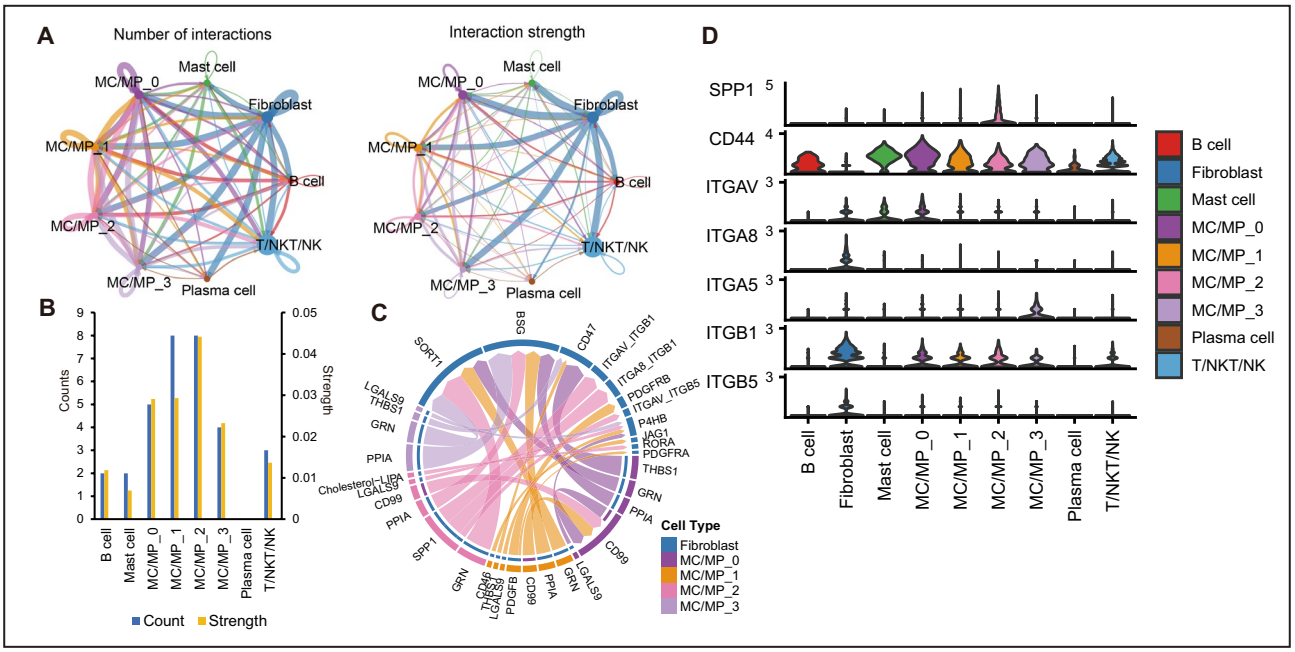

Figure 7. Ligand–receptor interaction analysis using scRNA-seq data from thrombi of patients with chronic thromboembolic pulmonary hypertension.

A, Network plots of the inferred numbers and strengths of ligand-receptor interactions. **B**, Inferred numbers and strengths of ligand–receptor interactions with fibroblasts based on cluster. Fibroblasts were set as receivers. **C**, Chord diagram visualizing all inferred ligand-receptor pairs from monocytes and macrophages subclusters to fibroblasts. **D**, Gene expression in the *SPP1* signaling pathway. scRNA-seq indicates single-cell RNA sequencing.

plasma concentration of osteopontin was higher in patients with atrial fibrillation than in those without and is correlated with the extent of atrial fibrosis.[69] Using unbiased proteomics, von Zur Mühlen et al showed that osteopontin levels in the urine can serve as a biomarker for venous thrombosis and pulmonary embolism.[70] It has also been reported that plasma osteopontin levels are higher among patients with venous thrombosis than in those without.[71] Osteopontin is cleaved by thrombin into 2 halves. In the present study, we showed that cleaved osteopontin (N-half) was present in a thrombus retrieved from a cerebral vessel. Considering that the presence of cleaved osteopontin implies a thrombogenic state, the level of osteopontin, especially cleaved osteopontin, in the peripheral blood may have potential value as a biomarker to predict intracardiac thrombus and future embolic events in patients with atrial fibrillation.

In the present study, thrombi retrieved from cerebral vessels were observed to contain neutrophils, consistent with previous studies.[67,72,73] However, neutrophils were not identified in the scRNA-seq data of thrombi harvested from patients with CTEPH. Experimental findings in a mouse inferior vena cava ligation model indicated that neutrophils are abundant in the initial stages of thrombus formation; however, their proportion decreased over time, with the proportion of monocytes and macrophages increasing at a later stage.[74] Therefore, neutrophils may disappear from the CTEPH thrombus with age.

This study has several limitations. First, some RINs were not sufficiently high in the thrombus samples. RINs in thrombus samples are commonly low, and acellular RINs tend to have lower RNA quantity and quality.[75] We selected samples with a relatively high RIN for RNA-seq and validated the results using quantitative polymerase chain reaction after adding other samples; however, the results should be carefully interpreted. Second, in the bulk RNA sequencing analysis, a larger sample size could have allowed for the detection of more subtle differences and enabled more refined analyses. Third, we were not able to analyze thrombi formed in arteries; thus, it remains to be confirmed in future studies whether our findings are applicable to arterial thrombi. Fourth, thrombus pathology may have been affected by mechanical manipulation during thrombectomy. Finally, the sample size of the clinical and immunohistochemistry data was not sufficient to analyze the effect of the thrombectomy procedure on thrombus features and may have been underpowered to detect differences in reperfusion quality.

In conclusion, our study identified transcriptional responses, including ECM formation, inflammatory response, and anti-inflammatory response, in thrombi. Collectively, our results indicate that *SPP1*-positive monocytes and macrophages play a key role in ECM formation

in thrombi and may be a potential target for novel antithrombotic therapies that modify thrombus maturation.

ARTICLE INFORMATION

Received July 9, 2025; accepted September 8, 2025.

Affiliations

Department of Neurology, Toyonaka Municipal Hospital, Osaka, Japan (T.K., Y.S., M.Y.); Department of Neurology (T.K., T.S., K.O., K.T., S.O., H.M.), Department of Immunology and Cell Biology (T.M.), Department of Pathology (T.M., M.K., E.M.) and Department of Neurosurgery, The University of Osaka Graduate School of Medicine, Osaka, Japan (H.N., H.K.), Department of Neurology, Osaka General Medical Center, Osaka, Japan (Y.S., M.S.); Department of Neurology, Osaka National Hospital, Osaka, Japan (S.O.); Department of Neurosurgery (J.I.) and Department of Pathology, Osaka General Medical Center, Osaka, Japan (K.S.), Department of Neurosurgery, Toyonaka Municipal Hospital, Osaka, Japan (M.N.) and Department of Neurology, National Hospital Organization, Osaka Toneyama Medical Center, Toyonaka, Japan (H.M.).

Sources of Funding

This study was supported by JSPS KAKENHI 21K15696 (T.K.) and the SENSHIN Medical Research Foundation 23–1-24 (T.S.).

Disclosures

The authors have no relevant financial or nonfinancial interests to disclose.

Supplemental Material

Tables S1–S3
Figures S1–S11

REFERENCES

1. Wendelboe AM, Raskob GE. Global burden of thrombosis. *Circ Res*. 2016;118:1340–1347. doi: 10.1161/CIRCRESAHA.115.306841
2. Tan KT, Lip GYH. Red vs white thrombi: treating the right clot is crucial. *Arch Intern Med*. 2003;163:2534–2535. doi: 10.1001/archinte.163.20.2534-a
3. Kamel H, Healey JS. Cardioembolic stroke. *Circ Res*. 2017;120:514–526. doi: 10.1161/CIRCRESAHA.116.308407
4. Hart RG, Pearce LA, Aguilar MI. Meta-analysis: antithrombotic therapy to prevent stroke in patients who have nonvalvular atrial fibrillation. *Ann Intern Med*. 2007;146:857–867. doi: 10.7326/0003-4819-146-12-200706190-00007
5. Kalathottukaren MT, Haynes CA, Kizhakkedathu JN. Approaches to prevent bleeding associated with anticoagulants: current status and recent developments. *Drug Deliv Transl Res*. 2018;8:928–944. doi: 10.1007/s13346-017-0413-4
6. Collins LJ, Silverman DI, Douglas PS, Manning WJ. Cardioversion of nonrheumatic atrial fibrillation. Reduced thromboembolic complications with 4 weeks of precardioversion anticoagulation are related to atrial thrombus resolution. *Circulation*. 1995;92:160–163. doi: 10.1161/01.cir.92.2.160
7. Jaber WA, Prior DL, Thamilarasan M, Grimm RA, Thomas JD, Klein AL, Asher CR. Efficacy of anticoagulation in resolving left atrial and left atrial appendage thrombi: a transesophageal echocardiographic study. *Am Heart J*. 2000;140:150–156. doi: 10.1067/mhj.2000.106648
8. Corrado G, Tadeo G, Beretta S, Tagliagambe LM, Manzillo GF, Spata M, Santarone M. Atrial thrombi resolution after prolonged anticoagulation in patients with atrial fibrillation. *Chest*. 1999;115:140–143. doi: 10.1378/chest.115.1.140
9. Lip GY, Hammerstingl C, Marin F, Cappato R, Meng IL, Kirsch B, van Eickels M, Cohen A; X-TRA study and CLOT-AF registry investigators. Left atrial thrombus resolution in atrial fibrillation or flutter: results of a prospective study with rivaroxaban (x-tra) and a retrospective observational registry providing baseline data (clot-af). *Am Heart J*. 2016;178:126–134. doi: 10.1016/j.ahj.2016.05.007
10. Kakkar VV, Howe CT, Flanc C, Clarke MB. Natural history of postoperative deep-vein thrombosis. *Lancet*. 1969;294:230–233. doi: 10.1016/S0140-6736(69)90002-6
11. Kearon C. Natural history of venous thromboembolism. *Circulation*. 2003;107:I-22-I-30. doi: 10.1161/01.CIR.0000078464.82671.78
12. Ribeiro A, Lindmarker P, Johnsson H, Juhlin-Dannfelt A, Jorfeldt L. Pulmonary embolism: one-year follow-up with echocardiography doppler and five-year survival analysis. *Circulation*. 1999;99:1325–1330. doi: 10.1161/01.cir.99.10.1325
13. Nicklas JM, Gordon AE, Henke PK. Resolution of deep venous thrombosis: proposed immune paradigms. *Int J Mol Sci*. 2020;21:2080. doi: 10.3390/ijms21062080
14. Nosaka M, Ishida Y, Kimura A, Kondo T. Time-dependent organic changes of intravenous thrombi in stasis-induced deep vein thrombosis model and its application to thrombus age determination. *Forensic Sci Int*. 2010;195:143–147. doi: 10.1016/j.forsciint.2009.12.008
15. Xie H, Kim K, Aglyamov SR, Emelianov SY, O'Donnell M, Weitzel WF, et al. Correspondence of ultrasound elasticity imaging to direct mechanical measurement in aging dvt in rats. *Ultrasound Med Biol*. 2005;31:1351–1359.
16. Mercado-Shekhar KP, Kleven RT, Aponte Rivera H, Lewis R, Karani KB, Vos HJ, Abruzzo TA, Haworth KJ, Holland CK. Effect of clot stiffness on recombinant tissue plasminogen activator lytic susceptibility in vitro. *Ultrasound Med Biol*. 2018;44:2710–2727. doi: 10.1016/j.ultrasmedbio.2018.08.005
17. Kitano T, Hori Y, Okazaki S, Shimada Y, Iwamoto T, Kanki H, Sugiyama S, Sasaki T, Nakamura H, Oyama N, et al. An older thrombus delays reperfusion after mechanical thrombectomy for ischemic stroke. *Thromb Haemost*. 2022;122:415–426. doi: 10.1055/a-1522-4507
18. Shimizu H, Hatakeyama K, Saito K, Shobatake R, Takahashi N, Deguchi J, Tokunaga H, Shimada K, Nakagawa I, Myochin K, et al. Age and composition of the thrombus retrieved by mechanical thrombectomy from patients with acute ischemic stroke are associated with revascularization and clinical outcomes. *Thrombosis Res*. 2022;219:60–69. doi: 10.1016/j.thromres.2022.09.004
19. Koge J, Hatakeyama K, Tanaka K, Yoshimoto T, Shiozawa M, Kondo Y, Sakamoto K, Kamogawa N, Abe S, Ishiyama H, et al. Thrombus age in ischemic stroke with atrial fibrillation: impact on mechanical thrombectomy. *Stroke Vasc Interv Neurol*. 2025;5:e001499. doi: 10.1161/SVIN.124.001499
20. Bolger AM, Lohse M, Usadel B. Trimmomatic: a flexible trimmer for illumina sequence data. *Bioinformatics*. 2014;30:2114–2120. doi: 10.1093/bioinformatics/btu170
21. Kim D, Langmead B, Salzberg SL. Hisat: a fast spliced aligner with low memory requirements. *Nat Methods*. 2015;12:357–360. doi: 10.1038/nmeth.3317
22. Liao Y, Smyth GK, Shi W. Featurecounts: an efficient general purpose program for assigning sequence reads to genomic features. *Bioinformatics*. 2013;30:923–930. doi: 10.1093/bioinformatics/btt656
23. Community TG. The galaxy platform for accessible, reproducible and collaborative biomedical analyses: 2022 update. *Nucleic Acids Res*. 2022;50:W345–W351.
24. Ge SX, Son EW, Yao R. Idep: an integrated web application for differential expression and pathway analysis of rna-seq data. *BMC Bioinformat*. 2018;19:534. doi: 10.1186/s12859-018-2486-6
25. Love MI, Huber W, Anders S. Moderated estimation of fold change and dispersion for rna-seq data with deseq2. *Genome Biol*. 2014;15:550. doi: 10.1186/s13059-014-0550-8
26. Szklarczyk D, Gable AL, Lyon D, Junge A, Wyder S, Huerta-Cepas J, Simonovic M, Doncheva NT, Morris JH, Bork P, et al. String v11: protein-protein association networks with increased coverage, supporting functional discovery in genome-wide experimental datasets. *Nucleic Acids Res*. 2019;47:D607–D613. doi: 10.1093/nar/gky1131
27. Chin CH, Chen SH, Wu HH, Ho CW, Ko MT, Lin CY. Cytohubba: identifying hub objects and sub-networks from complex interactome. *BMC Syst Biol*. 2014;8(Suppl 4):S11. doi: 10.1186/1752-0509-8-S4-S11
28. Wang X, Park J, Susztak K, Zhang NR, Li M. Bulk tissue cell type deconvolution with multi-subject single-cell expression reference. *Nat Commun*. 2019;10:380. doi: 10.1038/s41467-018-08023-x
29. Kwok AJ, Allcock A, Ferreira RC, Cano-Gamez E, Smee M, Burnham KL, Zurke YX; Emergency Medicine Research Oxford (EMROx), Novak A, Darwent M, et al. Neutrophils and emergency granulopoiesis drive immune suppression and an extreme response endotype during sepsis. *Nature Immunol*. 2023;24:767–779. doi: 10.1038/s41590-023-01490-5
30. Rittersma SZ, van der Wal AC, Koch KT, Piek JJ, Henriques JP, Mulder KJ, et al. Plaque instability frequently occurs days or weeks before occlusive coronary thrombosis: a pathological thrombectomy study in primary

percutaneous coronary intervention. *Circulation*. 2005;111:1160–1165. doi: 10.1161/01.CIR.0000157141.00778.AC
31. Viswanathan G, Kirshner HF, Nazo N, Ali S, Ganapathi A, Cumming I, Zhuang Y, Choi I, Warman A, Jassal C, et al. Single-cell analysis reveals distinct immune and smooth muscle cell populations that contribute to chronic thromboembolic pulmonary hypertension. *Am J Respir Crit Care Med*. 2023;207:1358–1375. doi: 10.1164/rccm.202203-0441OC
32. Hao Y, Stuart T, Kowalski MH, Choudhary S, Hoffman P, Hartman A, Srivastava A, Molla G, Madad S, Fernandez-Granda C, et al. Dictionary learning for integrative, multimodal and scalable single-cell analysis. *Nat Biotechnol*. 2024;42:293–304. doi: 10.1038/s41587-023-01767-y
33. Hafemeister C, Satija R. Normalization and variance stabilization of single-cell rna-seq data using regularized negative binomial regression. *Genome Biol*. 2019;20:296. doi: 10.1186/s13059-019-1874-1
34. Yu G, Wang LG, Han Y, He QY. Clusterprofiler: an r package for comparing biological themes among gene clusters. *OMICS*. 2012;16:284–287. doi: 10.1089/omi.2011.0118
35. Jin S, Plikus MV, Nie Q. Cellchat for systematic analysis of cell-cell communication from single-cell and spatially resolved transcriptomics. *Nature Protocols*. 2024;20:180–219.
36. DeRoo E, Zhou T, Yang H, Stranz A, Henke P, Liu B. A vein wall cell atlas of murine venous thrombosis determined by single-cell rna sequencing. *Communi Biol*. 2023;6:130. doi: 10.1038/s42003-023-04492-z
37. Campbell RA, Vieira-de-Abreu A, Rowley JW, Franks ZG, Manne BK, Rondina MT, Kraiss LW, Majersik JJ, Zimmerman GA, Weyrich AS. Clots are potent triggers of inflammatory cell gene expression: indications for timely fibrinolysis. *Arteriosclerosis, Thrombosis, Vascu Biol*. 2017;37:1819–1827. doi: 10.1161/ATVBAHA.117.309794
38. Wang Y, Reheman A, Spring CM, Kalantari J, Marshall AH, Wolberg AS, Gross PL, Weitz JI, Rand ML, Mosher DF, et al. Plasma fibronectin supports hemostasis and regulates thrombosis. *J Clin Invest*. 2014;124:4281–4293. doi: 10.1172/JCI74630
39. Momi S, Falcinelli E, Giannini S, Ruggeri L, Cecchetti L, Corazzi T, Libert C, Gresele P. Loss of matrix metalloproteinase 2 in platelets reduces arterial thrombosis in vivo. *J Exp Med*. 2009;206:2365–2379. doi: 10.1084/jem.20090687
40. Obradovic M, Zafirovic S, Soskic S, Stanimirovic J, Trpkovic A, Jevremovic D, Isenovic ER. Effects of igf-1 on the cardiovascular system. *Curr Pharm Des*. 2019;25:3715–3725. doi: 10.2174/1381612825666191106091507
41. Yin Y, Han Y, Shi C, Xia Z. Igf-1 regulates the growth of fibroblasts and extracellular matrix deposition in pelvic organ prolapse. *Open Med (Wars)*. 2020;15:833–840. doi: 10.1515/med-2020-0216
42. Fay WP, Parker AC, Condrey LR, Shapiro AD. Human plasminogen activator inhibitor-1 (pai-1) deficiency: characterization of a large kindred with a null mutation in the pai-1 gene. *Blood*. 1997;90:204–208. doi: 10.1182/blood.V90.1.204.204_204_208
43. Lok ZSY, Lyle AN. Osteopontin in vascular disease. *Arteriosclerosis, Thrombosis, Vascu Biol*. 2019;39:613–622. doi: 10.1161/ATVBAHA.118.311577
44. Lee GS, Salazar HF, Joseph G, Lok ZSY, Caroti CM, Weiss D, Taylor WR, Lyle AN. Osteopontin isoforms differentially promote arteriogenesis in response to ischemia via macrophage accumulation and survival. *Lab Investig*. 2019;99:331–345. doi: 10.1038/s41374-018-0094-8
45. Duvall CL, Weiss D, Robinson ST, Alameddine FMF, Guldberg RE, Taylor WR. The role of osteopontin in recovery from hind limb ischemia. *Arteriosclerosis, Thrombosis, Vascu Biol*. 2008;28:290–295. doi: 10.1161/ATVBAHA.107.158485
46. Koh A, da Silva AP, Bansal AK, Bansal M, Sun C, Lee H, et al. Role of osteopontin in neutrophil function. *Immunology*. 2007;122:466–475.
47. Dhanesha N, Nayak MK, Doddapattar P, Jain M, Flora GD, Kon S, Chauhan AK. Targeting myeloid-cell specific integrin α9β1 inhibits arterial thrombosis in mice. *Blood*. 2020;135:857–861. doi: 10.1182/blood.2019002846
48. Brill A. Integrin α9β1: a new target to fight thrombosis. *Blood*. 2020;135:787–788. doi: 10.1182/blood.2020004999
49. Nishimichi N, Higashikawa F, Kinoh HH, Tateishi Y, Matsuda H, Yokosaki Y. Polymeric osteopontin employs integrin alpha9beta1 as a receptor and attracts neutrophils by presenting a de novo binding site. *J Biol Chem*. 2009;284:14769–14776. doi: 10.1074/jbc.M901515200
50. Sabo-Attwood T, Ramos-Nino ME, Eugenia-Ariza M, Macpherson MB, Butnor KJ, Vacek PC, et al. Osteopontin modulates inflammation, mucin production, and gene expression signatures after inhalation of asbestos in a murine model of fibrosis. *Am J Pathol*. 2011;178:1975–1985. doi: 10.1016/j.ajpath.2011.01.048
51. Oono T, Specks U, Eckes B, Majewski S, Hunzelmann N, Timpl R, Krieg T. Expression of type vi collagen mrna during wound healing. *J Invest Dermatol*. 1993;100:329–334. doi: 10.1111/1523-1747.ep12470022
52. Theocharidis G, Drymoussi Z, Kao AP, Barber AH, Lee DA, Braun KM, Connelly JT. Type vi collagen regulates dermal matrix assembly and fibroblast motility. *J Invest Dermatol*. 2016;136:74–83. doi: 10.1038/JID.2015.352
53. McGuinness CL, Humphries J, Waltham M, Burnand KG, Collins M, Smith A. Recruitment of labelled monocytes by experimental venous thrombi. *Thromb Haemost*. 2001;85:1018–1024. doi: 10.1055/s-0037-1615957
54. Lin J, Guan M, Liao Y, Zhang L, Qiao H, Huang L. An old thrombus may potentially identify patients at higher risk of poor outcome in anterior circulation stroke undergoing thrombectomy. *Neuroradiology*. 2023;65:381–390. doi: 10.1007/s00234-022-03069-7
55. Ouyang JF, Mishra K, Xie Y, Park H, Huang KY, Petretto E, Behmoaras J. Systems level identification of a matrisome-associated macrophage polarisation state in multi-organ fibrosis. *elife*. 2023;12:e85530. doi: 10.7554/eLife.85530
56. Yang X, Liu Z, Zhou J, Guo J, Han T, Liu Y, Li Y, Bai Y, Xing Y, Wu J, et al. Spp1 promotes the polarization of m2 macrophages through the jak2/stat3 signaling pathway and accelerates the progression of idiopathic pulmonary fibrosis. *Int J Mol Med*. 2024;54:89. doi: 10.3892/ijmm.2024.5413
57. Morse C, Tabib T, Sembrat J, Buschur KL, Bittar HT, Valenzi E, Jiang Y, Kass DJ, Gibson K, Chen W, et al. Proliferating spp1/mertk-expressing macrophages in idiopathic pulmonary fibrosis. *Eur Respir J*. 2019;54:1802441. doi: 10.1183/13993003.02441-2018
58. Fu M, Shu S, Peng Z, Liu X, Chen X, Zeng Z, Yang Y, Cui H, Zhao R, Wang X, et al. Single-cell rna sequencing of coronary perivascular adipose tissue from end-stage heart failure patients identifies spp1(+) macrophage subpopulation as a target for alleviating fibrosis. *Arteriosclerosis, Thrombosis, Vascu Biol*. 2023;43:2143–2164. doi: 10.1161/ATVBAHA.123.319828
59. Hoeft K, Schaefer GJL, Kim H, Schumacher D, Bleckwehl T, Long Q, Klinkhammer BM, Peisker F, Koch L, Nagai J, et al. Platelet-instructed spp1+ macrophages drive myofibroblast activation in fibrosis in a cxcl4-dependent manner. *Cell Rep*. 2023;42:112131. doi: 10.1016/j.celrep.2023.112131
60. Hulsmans M, Schloss MJ, Lee IH, Bapat A, Iwamoto Y, Vinegoni C, Paccalet A, Yamazoe M, Grune J, Pabel S, et al. Recruited macrophages elicit atrial fibrillation. *Science*. 2023;381:231–239. doi: 10.1126/science.abq3061
61. Henderson NC, Arnold TD, Katamura Y, Giacomini MM, Rodriguez JD, McCarty JH, Pellicoro A, Raschperger E, Betsholtz C, Ruminski PG, et al. Targeting of αv integrin identifies a core molecular pathway that regulates fibrosis in several organs. *Nat Med*. 2013;19:1617–1624. doi: 10.1038/nm.3282
62. Murray IR, Gonzalez ZN, Baily J, Dobie R, Wallace RJ, Mackinnon AC, Smith JR, Greenhalgh SN, Thompson AI, Conroy KP, et al. Αv integrins on mesenchymal cells regulate skeletal and cardiac muscle fibrosis. *Nat Commun*. 2017;8:1118. doi: 10.1038/s41467-017-01097-z
63. Liaw L, Skinner MP, Raines EW, Ross R, Cheresh DA, Schwartz SM, Giachelli CM. The adhesive and migratory effects of osteopontin are mediated via distinct cell surface integrins. Role of alpha v beta 3 in smooth muscle cell migration to osteopontin in vitro. *J Clin Invest*. 1995;95:713–724. doi: 10.1172/JCI117718
64. Liaw L, Almeida M, Hart CE, Schwartz SM, Giachelli CM. Osteopontin promotes vascular cell adhesion and spreading and is chemotactic for smooth muscle cells in vitro. *Circ Res*. 1994;74:214–224. doi: 10.1161/01.RES.74.2.214
65. Wernig G, Chen SY, Cui L, Van Neste C, Tsai JM, Kambham N, et al. Unifying mechanism for different fibrotic diseases. *Proc Natl Acad Sci USA*. 2017;114:4757–4762. doi: 10.1073/pnas.1621375114
66. Furukoji E, Gi T, Yamashita A, Moriguchi-Goto S, Kojima M, Sugita C, Sakae T, Sato Y, Hirai T, Asada Y. Cd163 macrophage and erythrocyte contents in aspirated deep vein thrombus are associated with the time after onset: a pilot study. *Thrombosis J*. 2016;14:46. doi: 10.1186/s12959-016-0122-0
67. Laridan E, Denorme F, Desender L, Francois O, Andersson T, Deckmyn H, et al. Neutrophil extracellular traps in ischemic stroke thrombi: nets in stroke. *Ann Neurol*. 2017;82:223–232. doi: 10.1002/ana.24993

68. Patel M, Wei X, Weigel K, Gertz ZM, Kron J, Robinson AA, Trankle CR. Diagnosis and treatment of intracardiac thrombus. *J Cardiovasc Pharmacol*. 2021;78:361–371. doi: 10.1097/FJC.0000000000001064
69. Lin R, Wu S, Zhu D, Qin M, Liu X. Osteopontin induces atrial fibrosis by activating akt/gsk-3β/β-catenin pathway and suppressing autophagy. *Life Sci*. 2020;245:117328. doi: 10.1016/j.lfs.2020.117328
70. von Zur Mühlen C, Koeck T, Schiffer E, Sackmann C, Zürbig P, Hilgendorf I, Reinöhl J, Rivera J, Zirlik A, Hehrlein C, et al. Urine proteome analysis as a discovery tool in patients with deep vein thrombosis and pulmonary embolism. *Proteomics Clin Appl*. 2016;10:574–584. doi: 10.1002/prca.201500105
71. Memon AA, Sundquist K, PirouziFard M, Elf JL, Strandberg K, Svensson PJ, Sundquist J, Zöller B. Identification of novel diagnostic biomarkers for deep venous thrombosis. *Br J Haematol*. 2018;181:378–385. doi: 10.1111/bjh.15206
72. Tutino VM, Fricano S, Chien A, Patel TR, Monteiro A, Rai HH, Dmytriw AA, Chaves LD, Waqas M, Levy EI, et al. Gene expression profiles of ischemic stroke clots retrieved by mechanical thrombectomy are associated with disease etiology. *J Neurointerv Surg*. 2023;15:e33–e40. doi: 10.1136/neurintsurg-2022-018898
73. Ducroux C, Di Meglio L, Loyau S, Delbosc S, Boisseau W, Deschildre C, et al. Thrombus neutrophil extracellular traps content impair tpa-induced thrombolysis in acute ischemic stroke. *Stroke*. 2018;49:754–757. doi: 10.1161/STROKEAHA.117.019896
74. Nosaka M, Ishida Y, Kimura A, Kondo T. Time-dependent appearance of intrathrombus neutrophils and macrophages in a stasis-induced deep vein thrombosis model and its application to thrombus age determination. *Int J Legal Med*. 2009;123:235–240. doi: 10.1007/s00414-009-0324-0
75. Tutino VM, Fricano S, Frauens K, Patel TR, Monteiro A, Rai HH, et al. Isolation of rna from acute ischemic stroke clots retrieved by mechanical thrombectomy. *Genes (Basel)*. 2021;12:1617. doi: 10.3390/genes12101617